IEEE Access
Multidisciplinary | Rapid Review | Open Access Journal

Received August 7, 2020, accepted August 11, 2020, date of publication August 14, 2020, date of current version September 2, 2020.

Digital Object Identifier 10.1109/ACCESS.2020.3016649

Compact Sub-6-GHz Four-Element MIMO Slot Antenna System for 5G Tablet Devices

SHU-CHUAN CHEN[1], (Member, IEEE), LUNG-CHI CHOU[2], CHUNG-I. G. HSU[3], (Member, IEEE), AND SHENG-MIN LI[1]

[1]Electrical and Electronic Engineering Department, Chung Cheng Institute of Technology, National Defense University, Taoyuan 335, Taiwan
[2]Electrical Engineering Department, National Yunlin University of Science and Technology, Douliu 640, Taiwan
[3]Electronic Systems Research Division, National Chung-Shan Institute of Science and Technology, Taoyuan 325, Taiwan

Corresponding author: Shu-Chuan Chen (scchen0319@gmail.com)

This work was supported by the Ministry of Science and Technology, Taiwan, under Grant MOST 107-2221-E-606-004.

ABSTRACT A sub-6-GHz four-element multi-input multi-output (MIMO) slot antenna system was proposed in this study for fifth-generation (5G) tablet computers, where each antenna element was constructed using a slot structure. To effectively use the available space in a tablet and maximize the screen, we have deployed the MIMO antenna system on the left side-edge frame of the tablet. The MIMO antenna system measuring 37.2×7 mm^2 consists of two identical 13.6×7 mm^2 dual-slot-antenna units that are separated by 10 mm. The two closely spaced slot antennas in the same dual-slot-antenna unit are arranged asymmetrically mirrored of each other with respect to the system ground plane. Although the dual-slot-antenna unit is very compact, the isolation between the two slot antennas in the same unit can be enhanced by using an ungrounded full-wavelength strip resonator. With the two ungrounded resonators in the MIMO slot antenna system, the simulated intra-unit isolations at the mid-band frequency can be enhanced by about 3.5 dB to meet the design requirement. As a byproduct, the two ungrounded resonators in the MIMO antenna system can also enhance the simulated mid-band antenna efficiency by about 4.5% and lower the worst simulated ECC by 0.195, from 0.518 to 0.323. This MIMO antenna system can support the frequency band of 3400–3600 MHz for 5G. In the operating band, the measured isolation is larger than 11 dB, and the measured antenna efficiency is larger than 40%. The envelope correlation coefficients (ECCs) calculated from the measured complex E-field radiation patterns are all smaller than 0.23, making the proposed design suitable for 5G mobile communications that require fast transmission.

INDEX TERMS Tablet antennas, multi-input multi-output (MIMO) antennas, slot antennas, miniaturized antennas, 5G MIMO antenna system, envelope correlation coefficient (ECC).

I. INTRODUCTION

The desire for a high data-transmission rate in the fifth-generation (5G) mobile communications has fueled the need for the multiple-input multiple-output (MIMO) antenna systems that can provide large transmission volumes and high transmission rates. For a 5G mobile communication device, the development trends of light weight, compact appearance, and large screens with a high display-to-body ratio should be seriously considered by engineers. The trends in device appearance create the challenge of deploying an antenna in a more and more limited space. On the other hand, a 5G antenna system usually consists of more antenna elements than does a fourth-generation (4G) one, an outcome further raising the design challenge of how to incorporate multiple antennas in a confined space while keeping good isolation between individual antennas.

Many densely deployed MIMO antenna systems have been proposed for mobile communications in recent years [1]–[12]. Although these MIMO antenna systems are mounted on some different mobile communication devices, the design goal of incorporating in a limited space as many antenna elements as possible for faster transmission is the same. For that purpose, several different schemes for optimizing isolation between antenna elements have been presented. In [1]–[3], the antenna elements in a 5G MIMO antenna system mounted in a smart phone were spaced by a distance of as large as 10–30 mm. For two-element MIMO antenna

The associate editor coordinating the review of this manuscript and approving it for publication was Sotirios Goudos.

systems, a decoupling inductor was added between one branch terminal of the first antenna and that of the second antenna in a tablet computer [4] and in a notebook computer [5]; a chip capacitor was used in the common short-circuit route of two loop antennas in a tablet computer [6]. In these compact antenna systems, good isolation can be achieved even without an extra physical space between the two antenna elements. Alternatively, the two antennas can be chosen to have different structures, one being an inverted-F metal strip and the other an L-shaped slot, such that the mutual coupling in between is minimized. Such an example can be found in [7], where in a tablet computer the two antennas with a profile height of only 4 mm can be separated by a gap of only 2 mm without using any additional reactive chip elements to achieve good isolation in the 5G operating band of 3400–3800 MHz. It is quite often that two antennas with a small gap are grouped into a dual-antenna unit, which in turn serves as the building block for constructing a MIMO antenna system consisting of more than two antenna elements [8]–[10]. The two elements of the dual-antenna units in [8] and [9] are on the two sides of the system ground plane with no physical gap in the direction along the antenna's main metal strip and are asymmetrically mirrored of each other, whereas those in [10] are on the same side of the system ground plane and are mirrored of each other with a small gap of only 3 mm. All these three MIMO antenna systems are configured on the 7-mm-wide side-edge frame of a smartphone so as to maximize the display screen. However, this maximization is slightly limited by the required 1-mm-wide clearance area in the system ground plane. In the three dual-antenna units in [8]–[10], a short-circuit decoupling technique was adopted to enhance the intra-unit isolation.

To date, the two closely spaced antenna elements comprising a dual-antenna unit are all made of metal strips [8]–[10]. These dual-antenna units can serve as the building blocks for constructing a massive MIMO antenna system. By contrast, dual-antenna units consisting of two closely spaced slot antennas have not been found yet, to the best of the authors' knowledge. This might be because the magnetic coupling between two closely spaced slots etched from the same metal plane is large and is not easy to reduce. Since slot antennas feature the ease of integrating with metal surroundings and hence are suitable to be mounted on devices with a metal frame or back cover, it is worthwhile to design a dual-antenna unit consisting of only slot antennas. For distinction purpose, we will call this unit a dual-slot-antenna unit. If the two slot antennas in the same unit are very close to each other, the isolation in between may be a serious issue. Literature review reveals that dual-slot-antenna units have not been proposed for tablet applications yet, not mentioning how to enhance the intra-unit isolation when the two slot antennas in the same unit are very close to each other.

In this article, we propose for tablet computers a 5G MIMO antenna system consisting of two dual-slot-antenna units, each being composed of two closely spaced slot antennas. The MIMO antenna system is deployed on the left side-edge frame of a tablet. The two dual-slot-antenna units, each measuring only 13.6×7 mm^2, are identical and are separated by an edge-to-edge distance of only 10 mm. The resulting 5G four-element MIMO antenna system with the separation distance included occupies an area of only 37.2×7 mm^2. In the same dual-slot-antenna unit, the two slots are on the two opposite sides of the system ground plane and are asymmetrically mirrored of each other with respect to the same ground plane. Unlike in [8]–[10] where a 1-mm-wide ground clearance exists between the FR4 substrate and the system ground plane, our proposed MIMO antenna system does not require any ground clearance and hence is well suited for tablets with a very large display-to-body ratio.

In this four-element MIMO antenna system, each individual slot antenna can produce an operating band that is wide enough to cover 3400–3600 MHz for 5G. Two ungrounded full-wavelength strip resonators are employed to enhance the simulated intra-unit isolations by about 3.5 dB at the mid-band frequency. In the operating band of the four-element MIMO antenna system, the measured in-band isolation is larger than 11 dB. The envelope correlation coefficients (ECCs) calculated from the measured complex E-field radiation patterns are all smaller than 0.23. When only one antenna is excited and all other three are silent, the measured antenna efficiency is greater than 40%.

II. PROPOSED MIMO ANTENNA SYSTEM DESIGN

A. MIMO ANTENNA SYSTEM STRUCTURE

Figure 1 shows the layout of the 5G four-element MIMO antenna system, which is constructed on a 9.7'' tablet computer. The 200×150 mm^2 system ground plane and the perpendicularly surrounding 7-mm-wide side-edge frame are made of 0.2-mm-thick copper. The proposed MIMO antenna system is constructed on the left section of the side-edge frame (or called the left side-edge frame for short), which for fabrication convenience is replaced by a 150×7 mm^2

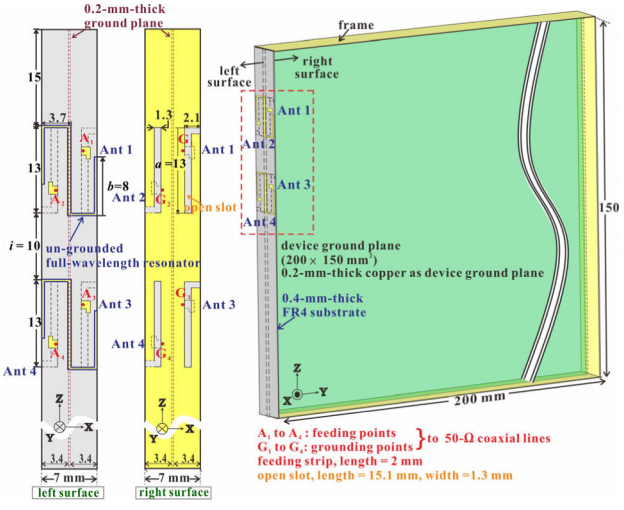

FIGURE 1. Structural view of the MIMO antenna system and details.

FR4 substrate of thickness 0.4 mm, dielectric constant (ε_r) 4.4, and loss tangent 0.02. The metal printed on the right surface of the FR4 substrate is connected to the tablet's system ground plane and is soldered to the upper and lower sections of the side-edge frame, respectively, around the upper-left and lower-left corners of the system ground plane. This surface hence becomes part of the inner surface of the side-edge frame surrounding the tablet's system ground plane. To distinguish this surface from the system ground plane, we will call the former the ground plane of the FR4 substrate.

The proposed 5G MIMO antenna system is placed 15 mm below the upper end of the left side-edge frame. Its four antenna elements are named from Ant 1 to Ant 4, where Ants 1 and 2 form the first dual-slot-antenna unit and Ants 3 and 4 form the second. The two dual-slot-antenna units have the same structure and size, each measuring 13.6×7 mm^2, and are separated by an edge-to-edge distance of 10 mm. Hence, the whole 5G MIMO antenna system occupies an area of 37.2×7 mm^2. Detailed geometry of the first dual-slot-antenna unit and the relevant operation mechanism will be addressed in what follows.

The two slot antennas, Ants 1 and 2, in the first unit are arranged to be asymmetrically mirrored of each other with respect to the system ground plane (alternatively, the geometry of the first unit can be said to be rotationally symmetric). Two L-shaped open-ended slots, one for Ant 1 and the other for Ant 2, are etched from the ground plane of the FR4 substrate, as shown in Figure 1. With the crude approximation of the effective dielectric constant $\varepsilon_{r,\text{eff}} = 2\varepsilon_r/(1 + \varepsilon_r)$ [13] in mind for slot structures, the length of the open-ended slot corresponding to a quarter wavelength at the center operating frequency of 3.5 GHz is initially chosen to be 16.7 mm. Structural fine-tuning process in the design leads to an open-ended slot of width 1.3 mm and length 15.1 mm, which is close to the initially selected length of 16.7 mm.

Each slot can be excited by a 2-mm-long L-shaped metal strip on the opposite surface (i.e. the left surface) of the FR4 substrate to produce a quarter-wavelength resonance mode. For Ant 1, the center conductor of the feeding mini-coaxial cable penetrates the FR4 substrate from its right surface and is connected with this L-shaped metal strip at point A_1, and the outer shield of the cable is connected with the ground plane of the FR4 substrate at point G_1. A 0.3-mm-wide, 36-mm-long double-hook-shaped strip on the left surface of the substrate behaves as an ungrounded full-wavelength resonator. Two ungrounded narrow strip resonators in the MIMO antenna system can enhance the simulated intra-unit isolations by about 3.5 dB at the mid-band frequency. Note that the resonator length of 36 mm is not too far away from the empirically estimated length of 47.56 mm for the ideal one-wavelength straight microstrip resonator at 3.5 GHz [14, eqs. (6.21)–(6.23)].

B. EXPERIMENT AND MEASUREMEMT RESULTS

Figure 2 shows the photos of the 5G four-element MIMO antenna system in the presence of the tablet viewed from two different angles. Figure 3 presents the left- and right-surface photos of the FR4 substrate alone. Note that the right-surface photo has been flipped left to right for easy perception of the antenna structure. The software tool ANSYS HFSS (Version 15) [15] was used for simulation, and the simulated and measured S-parameters are presented in Figures 4 and 5, respectively. The relevant curves in these two figures appear to have similar trends. The criterion chosen for the impedance-matched operating band is that the reflection coefficients must be equal to or smaller than –6 dB (i.e., VSWR $\leq$ 3). Figures 4 and 5 show that the operating band of the proposed MIMO antenna system can

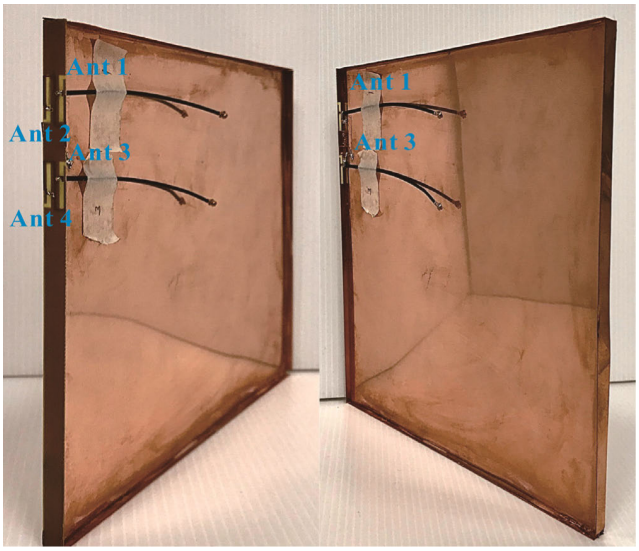

FIGURE 2. Photo of 5G four-antenna system on a tablet.

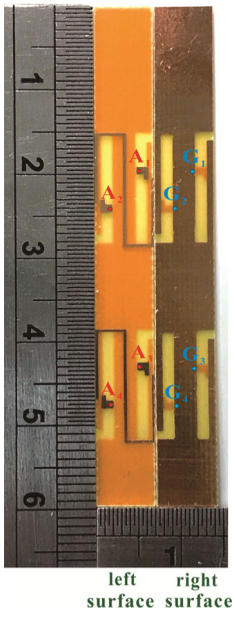

FIGURE 3. Left-surface photo and left-right-flipped right-surface pho to of the FR4 substrate alone.

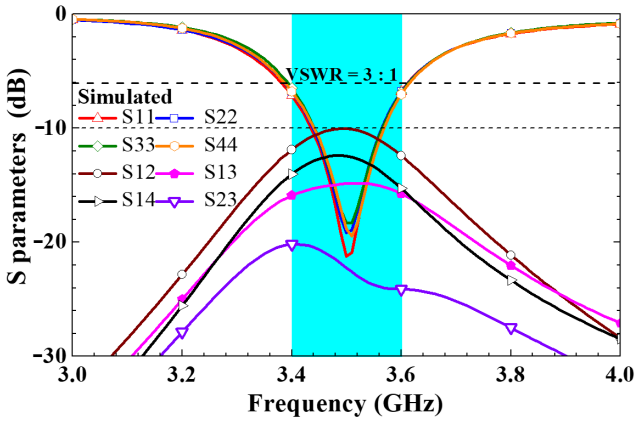

FIGURE 4. Simulated *S*-parameters of the 5G MIMO antenna system.

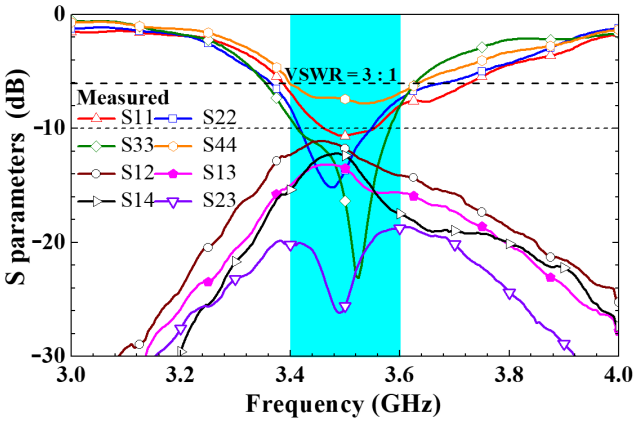

FIGURE 5. Measured *S*-parameters of the 5G MIMO antenna system.

cover the desired 3400–3600 MHz band for 5G communications. Within the operating band, the transmission coefficients between antennas must be equal to or less than –10 dB for the system to be considered to have good isolation, a criterion also adopted by many other papers ([9], for example). From this criterion, the proposed 5G MIMO antenna system can be regarded as having good isolation since the simulated and measured transmission coefficients in Figures 4 and 5 are all smaller than –10 dB and –11 dB, respectively. The measured results slightly differ from the simulated ones. The discrepancies could be due to the fact that the additional mini coaxial cables and IPEX-to-SMA adaptors used in measurement are not considered in simulation. Moreover, the parameter variation of the FR4 substrate and the imperfection in fabrication could also be part of the reasons for the discrepancies.

Besides isolation, the ECC is another important parameter to present for a MIMO antenna system [16]. Generally speaking, ECC $<$ 0.5 is a criterion suitable for practical applications [17]. Figure 6 shows the ECCs calculated from the complex E-field radiation patterns simulated and measured for the 5G MIMO antenna system. The ECCs simulated and measured for the system in the 3400–3600 MHz frequency band for 5G are smaller than 0.323 and 0.23,

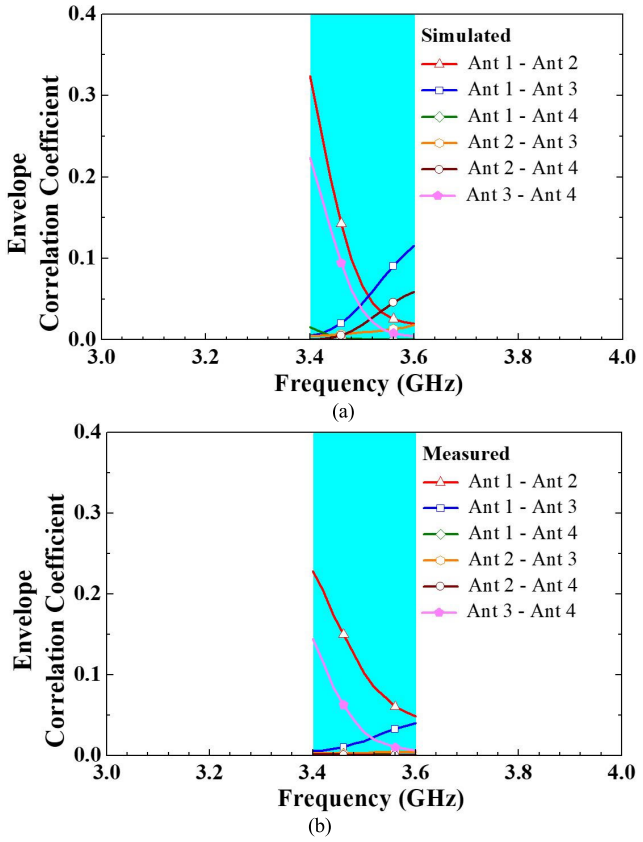

FIGURE 6. ECCs calculated from the complex E-field radiation patterns (a) simulated and (b) measured for the 5G MIMO antenna system.

respectively. They are all below the recommended upper bound of 0.5, proving that good channel independence exists between antenna elements in the proposed 5G MIMO antenna system.

The four-antenna system was built by separating two dual-slot-antenna units with an appropriate edge-to-edge spacing. Figure 7 shows at 3500 MHz the three-dimensional

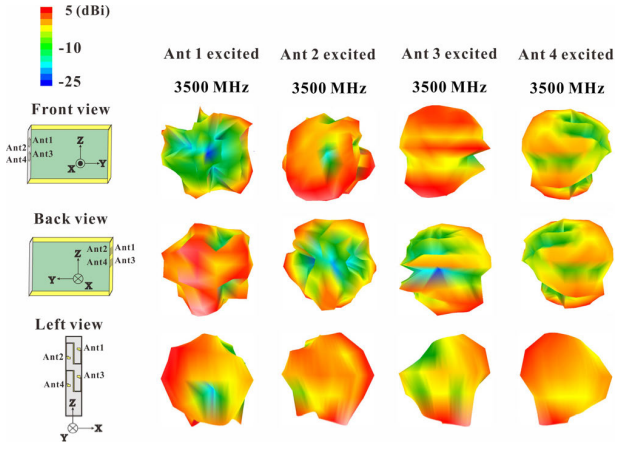

FIGURE 7. Measured far-field radiation patterns of the 5G MIMO antenna system.

far-field radiation patterns when only one of the four antennas is excited and the other three are terminated in a 50-ohm load. This figure shows that the radiated fields of these antenna elements when excited alone have very dissimilar patterns. This is the reason why the ECCs calculated from the measured complex E-field radiation patterns are smaller than 0.23 in Figure 6. The measured antenna efficiency shown in Figure 8 ranges from 40% to 53% within the 3.4–3.6 GHz frequency band, which meets the need of MIMO applications for 5G [18].

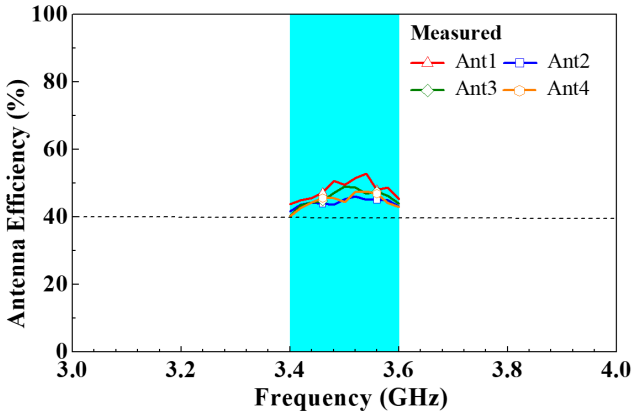

FIGURE 8. Measured antenna efficiency of the 5G MIMO antenna system.

C. COMPARISON STUDY

In this subsection, we will compare the S-parameters of the MIMO antenna system without and with the ungrounded full-wavelength strip resonators. Figures 9 and 10 show the simulated reflection and transmission parameters, respectively. Obviously, the operating bands for both cases (without and with the ungrounded strip resonators) can cover the desired 3400–3600 MHz required by 5G. Without the ungrounded double-hook-shaped full-wavelength strip resonators, the impedance match is better (i.e., $|S_{11}|$, $|S_{22}|$, $|S_{33}|$, and $|S_{44}|$ are smaller) and the operating band is wider. In general, the magnetic coupling predominates over the electric coupling between two coplanar open-ended quarter-wavelength slot antennas whose open ends are not facing each other and are not very close to each other. For the open-ended resonant slots in the MIMO antenna system, the maximum E-field (H-field) occurs around the open-end (short-end) of a slot. It is of no surprise that among the four inter-unit transmission coefficients (i.e., $|S_{13}|$, $|S_{14}|$, $|S_{23}|$, and $|S_{24}|$) in Figure 10, $|S_{14}| > |S_{13}| > |S_{23}|$ because the distance between the two short-ends of Ants 1 and 4 is smaller than that of Ants 1 and 3, which in turn is smaller than that of Ants 2 and 3. In addition, $|S_{13}|$ is very close to $|S_{24}|$ because the distance between the two short-ends of Ants 1 and 3 is the same as that of Ants 2 and 4. Although the inter-unit transmission coefficients are all smaller than –10 dB, the intra-unit transmission coefficients (i.e., $|S_{12}|$ and $|S_{34}|$) are both larger than –10 dB in the operating band. In addition, the simulated

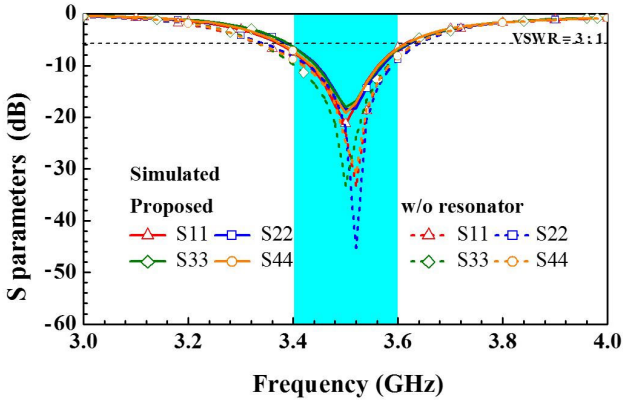

FIGURE 9. Simulated reflection coefficients of the 5G MIMO antenna system without and with the ungrounded resonator.

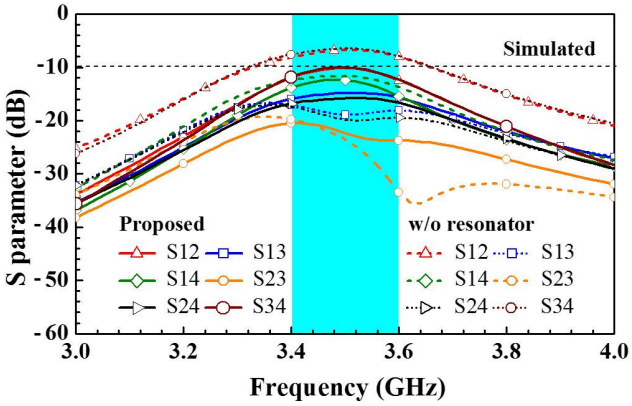

FIGURE 10. Simulated transmission coefficients of the 5G MIMO antenna system without and with the ungrounded resonator.

intra-unit isolations at 3.5 GHz (the mid-band frequency) for the first and second dual-slot-antenna units are as small as only 6.67 and 6.43 dB, respectively. These results are undesirable. Fortunately, this trouble can be conquered by using the proposed ungrounded strip resonators. In the presence of the ungrounded resonators, although the impedance match degrades such that the operating band is slightly narrowed, the intra-unit transmission coefficients are decreased to below –10 dB in the entire operating band. The simulated intra-unit isolations at 3.5 GHz are enhanced by about 3.44 and 3.58 dB with the smallest isolation of about 10.11 and 10.01 dB for first and second dual-slot-antenna units, respectively. The average enhancement in the intra-unit isolation at 3.5 GHz is about 3.5 dB. Note that the ungrounded resonators also slightly enhance the mid-band inter-unit isolation between Ants 1 and 4 by about 0.7 dB, but they degrade the isolations between Ants 1 and 3, between Ants 2 and 4, and between Ants 2 and 3. Although that is the case, the resulting $|S_{13}|$, $|S_{24}|$, and $|S_{23}|$ are still below –10 dB. In short, the ungrounded strip resonators trade a wider operating band for a narrower but still acceptable one and, most importantly,

satisfying isolations, which are desirable results making the dual-slot-antenna units meet the MIMO operation criteria.

Having seen the effects of the ungrounded resonators on the S-parameters, we can further simulate the antenna efficiency and ECC. Figures 11 shows that the simulated antenna efficiencies for the MIMO antenna system without and with the two ungrounded resonators. Obviously, the ungrounded resonators not only enhance the intra-unit isolations, but also raise the mid-band antenna efficiency by 4.5%. Assuming Ant 1 is excited with all other antenna elements silent, we summarize from Figures 9, 10 and 11 into Table 1 the ratios of the power reflected, transmitted, radiated, and dissipated internally to the power incident onto the input port of Ant 1 at 3.5 GHz. In this table, 0.48% (0.75%) and 21.03% (9.74%), the ratios of the power reflected from port 1 and transmitted to port 2 for the case without (with) the ungrounded resonators, are converted from $|S_{11}| = -23.22$ dB (–21.25 dB) and $|S_{21}| = -6.77$ dB (–10.11 dB), respectively. The ratios of the power transmitted to ports 3 and 4 can be obtained in a similar manner. The ratio of the power radiated can be read from Figure 11. Furthermore, the ratio of the power dissipated internally is computed according to the power conservation, i.e., 1 minus the ratios of the power reflected, transmitted, and radiated. Without the ungrounded resonators, more than 20% and 6% of the power incident onto Ant 1 are coupled to the ports of Ants 2 and 4, respectively, leaving 41.19% radiated and only 1.28% coupled to the port of Ant 3. With the ungrounded resonators, the powers coupled to the ports of Ants 2 and 4 are reduced, and the powers radiated and coupled to the port of Ant 3 are both increased. From the above observation, the ungrounded resonator in the first dual-slot-antenna unit may be heuristically regarded as a wave-trapping component that reduces the coupling from Ant 1 to Ant 2. The power trapped by this ungrounded resonator is partially radiated, partially dissipated in the resonator itself, partially coupled to the ungrounded resonator in the second dual-slot-antenna unit (or called the second ungrounded resonator for short), and partially coupled to the four slot antennas. The power incident onto port 1 can be coupled directly to the other antenna ports through the direct slot-slot coupling and through the indirect slot-slot-slot, slot-resonator-slot, and slot-resonator-resonator-slot couplings. Signals coupled from Ant 1 to any other antenna may come from several different coupling paths, the relation between which may be constructive or destructive. The results shown in Figure 10 and Table 1 are due to the net coupling effects. In short, the antenna efficiencies and internal losses have both slightly increased in the presence of the ungrounded resonators.

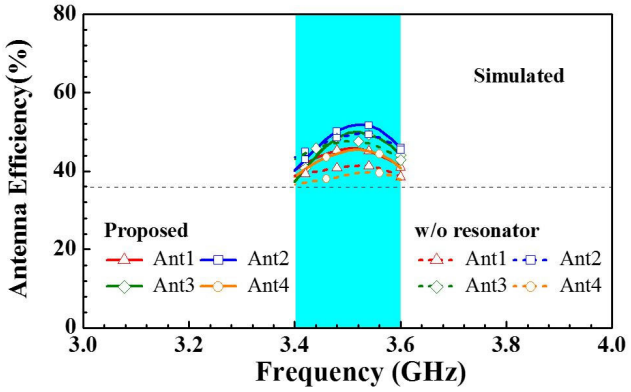

FIGURE 11. Simulated antenna efficiency of the 5G MIMO antenna system without and with the ungrounded resonators.

TABLE 1. The ratios of power reflected, transmitted, radiated, and dissipated internally to the power incident onto port 1 at 3.5 GHz.

ratio of power	without ungrounded resonators	with ungrounded resonators
reflected from port 1	0.48%	0.75%
transmitted to port 2	21.03%	9.74%
transmitted to port 3	1.28%	3.30%
transmitted to port 4	6.81%	5.78%
radiated	41.19%	45.75%
dissipated internally	29.21%	34.68%

At this juncture, one might think that it is unreasonable to have shallow dips in the $|S_{13}|$ and $|S_{23}|$ curves without the ungrounded resonators in Figure 10. This is true for a two-port device consisting of only two coupled resonators. For a multi-port device consisting of more than two resonators, the statement that a dip should not appear in a transmission-coefficient curve may no longer be true. As a verification, we simulate the transmission coefficient for the MIMO antenna system consisting of only Ants 1 and 3 (Ants 2 and 3) without any ungrounded resonators; the bell-shaped $|S_{13}|$ ($|S_{23}|$) curve indeed does not have a dip, as expected. However, if we add Ant 4 to the system, we will find a shallow dip appears in the $|S_{13}|$ ($|S_{23}|$) curve. For conciseness, relevant figures on these simulated results are omitted here.

Figure 12 shows the ECC data for the MIMO antenna system without and with the ungrounded resonators. Without the ungrounded resonators, the worst simulated in-band ECC occurs at 3.4 GHz for the pair of Ants 1 and 2 and is 0.518, which can be lowered to 0.323 for the case with the ungrounded resonators. This implies that the ungrounded resonators in the MIMO antenna system can help lower the worst ECC by 0.195. Although the worst simulated intra-unit ECC of 0.323 for the pair of Ants 1 and 2 is well below the practical criterion of 0.5 mentioned in the paragraph addressing Fig. 6, it is still larger than the more stringent ECC criterion of 0.3 that many researchers prefer to use. If this more stringent ECC criterion is adopted, our proposed structure should be modified to further lower the ECCs. This can be achieved by shifting Ant 2 upward by, say, 3 mm. In the

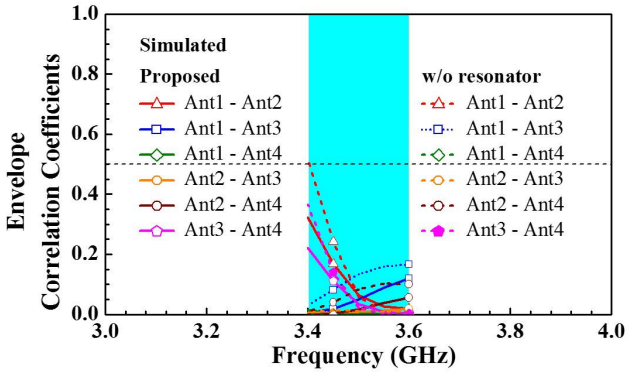

FIGURE 12. Simulated ECCs of the 5G MIMO antenna system without and with the ungrounded resonators.

process, the first ungrounded resonator of the same length is deformed such that the first dual-slot-antenna unit maintains its rotational symmetry in geometry and the ungrounded resonator still passes over the two short-ends of Ants 1 and 2. In addition, all other structural parameters remain unchanged. Figure 13 shows that, by doing so, the simulated ECC for the pair of Ants 1 and 2 at 3.4 GHz is indeed lowered from a slightly higher value of 0.323 to an acceptable value of 0.219, but with the paid price of a larger circuit area.

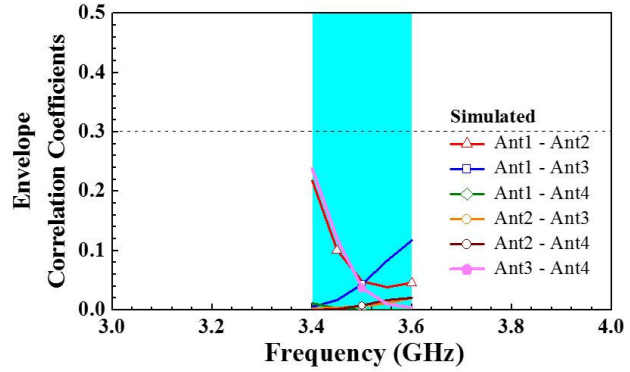

FIGURE 13. Simulated ECCs for the 5G MIMO antenna system with Ant 2 shifted upward by 3 mm.

From Figure 10 and Table 1, it is seen that the ungrounded resonators can significantly enhance the isolation between the two antenna elements in the same dual-slot-antenna unit. Although they also degrade the isolation between Ants 1 and 3 and that between Ants 2 and 3, these two isolation levels are still larger than that between the two intra-unit antenna elements. Hence, for simplicity and for digging deeper how the resonators affect the isolation performance, we will consider the case where only the first dual-slot-antenna unit is present and show the E-fields in the slots and the surface electric currents on the metal part. We will first simulate and compare the E-fields in the slots at 3.5 GHz for the two cases: without and with the ungrounded resonator. They are shown in Figure 14. When Ant 1 (2) is excited with Ant 2 (1) silent in the absence of this resonator, the E-field is strongly distributed in the quarter-wavelength slot

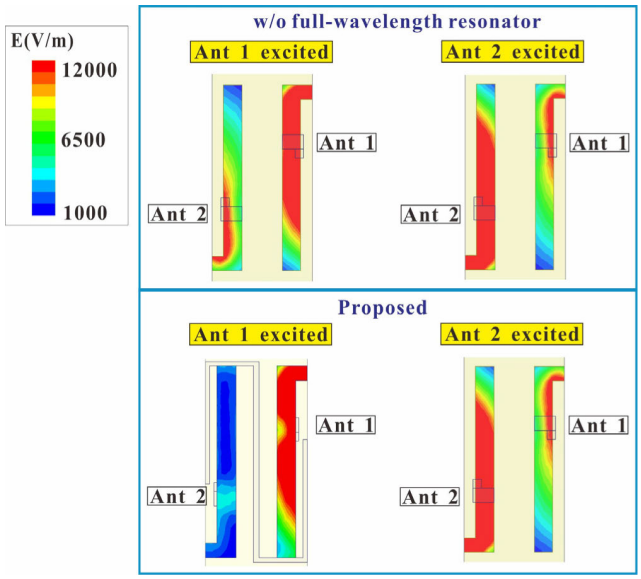

FIGURE 14. Simulated E-field distributions in the two slots of the 5G two-element MIMO antenna system without and with the ungrounded resonator at 3.5 GHz.

of Ant 1 (2) and is weaker but still measurable in the slot of Ant 2 (1). In the presence of this resonator, the E-field in the slot of the excited antenna remains strong, but that in the slot of the silent antenna becomes negligibly weak and almost non-measurable. These observations indicate that the ungrounded strip resonator can greatly reduce the coupling from the excited antenna to the silent antenna within the same dual-slot-antenna unit.

Next, we simulate and compare the surface electric currents on the two slots' surrounding metal at 3.5 GHz for the same two cases. Figure 15 presents such results. Without the

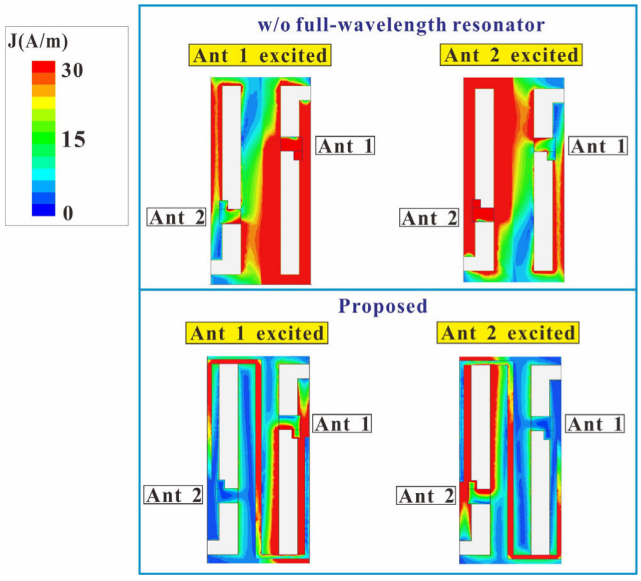

FIGURE 15. Simulated surface electric currents on the surrounding metal of the slots in the 5G two-element MIMO antenna system without and with the ungrounded resonator at 3.5 GHz.

ungrounded resonator, surface electric currents are found to flow around the slots of both excited and silent antennas, with weak but measurable electric current on the L-shaped metal strip in the silent antenna. In the presence of this resonator, surface electric currents flow mainly around the slot of the excited antenna and on the ungrounded resonator. The electric current flowing around the silent antenna's slot is much weaker, and that on the corresponding L-shaped metal strip is even negligibly weak. Note that the surface electric-current patterns indicate that the ungrounded double-hook-shaped strip is in full-wavelength resonance, and the strength of the electric current on the silent antenna's L-shaped metal strip can be regarded as proportional to the coupling from the excited antenna to the silent antenna. Hence, the surface electric currents shown in this figure serve as another proof that the ungrounded full-wavelength strip resonator can effectively improve the intra-unit isolation.

D. PARAMETRIC STUDIES

In this subsection, we will perform some parametric studies in order to dig deeper the operation mechanisms of the proposed MIMO antenna system. The first parameter to be studied is the edge-to-edge distance i between the two dual-slot-antenna units for better understanding how this distance influences the isolation. Figures 16 and 17 provide the simulated reflection and transmission coefficients, respectively, for three different values of i, i.e., 5, 10, and 15 mm. It is obvious from the reflection coefficients given in Figure 16 that all four antennas can cover the desired 3400–3600 MHz band required by 5G for the three different separation distances. Figure 17 shows the same set of the intra-unit transmission coefficient $|S_{12}|$ and inter-unit ones $|S_{13}|$, $|S_{14}|$, and $|S_{23}|$ as in Figures 4 and 5. Clearly, within the operating band, the $|S_{12}|$ values are relatively large. This is because Ants 1 and 2 are very close to each other. In contrast, the $|S_{23}|$ values within the operating band are relatively small. This may be because the short-ends of the slots in Ants 2 and 3 are the farthest among the four two-antenna pairs. When in resonance, these short-ends of the slots are the places where the H-fields are maximum, and the magnetic coupling could be the dominant coupling scheme in the slot structure. Hence, the coupling between Ants 2 and 3 is weak even if i is set to only 5 mm, for the distance between the short-ends of the slots in Ants 2 and 3 is still large. For the other two cases pertaining to $|S_{13}|$ and $|S_{14}|$, the distances between the associated short-ends of the slots are intermediate, and thus the $|S_{13}|$ and $|S_{14}|$ values are between the $|S_{12}|$ and $|S_{23}|$ values. Close scrutiny of Figure 17 reveals that the worst in-band inter-unit isolation occurs for $|S_{14}|$ and is 12, 12.2, 13.5 dB, respectively, for $i = 5$, 10, and 15 mm. To keep the four-element MIMO antenna system compact enough while preserving reasonably high inter-unit isolations, we can select $i = 5$ mm in our design. However, this selection corresponds to a worst intra-unit isolation ($-20\log_{10}|S_{12}|$) of 9.8 dB, which is undesirable. Hence, $i =$ 10 mm associated with the worst intra-unit isolation of 10 dB

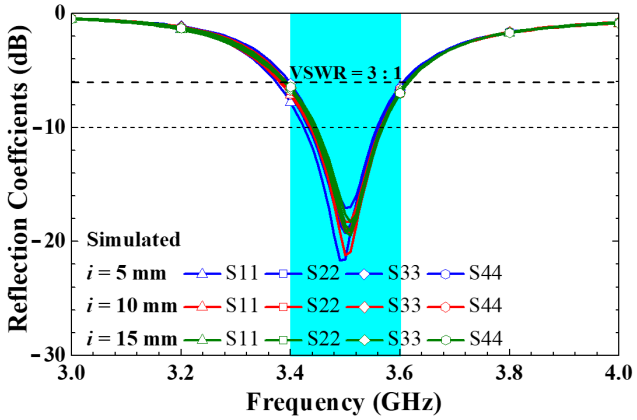

FIGURE 16. Simulated reflection coefficients of the 5G MIMO antenna system for different values of *i*.

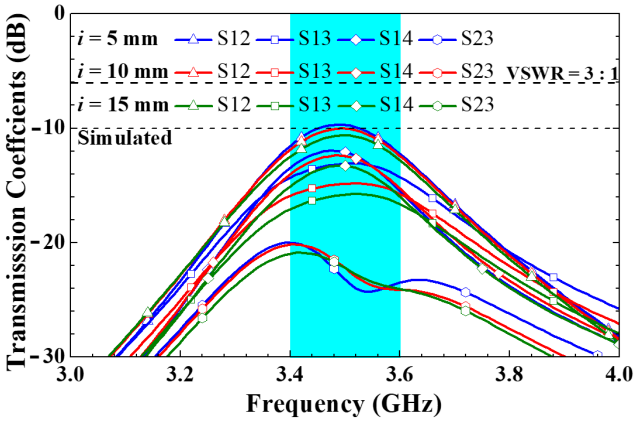

FIGURE 17. Simulated transmission coefficients for different values of *i*.

is chosen to be the spacing between the two dual-slot-antenna units.

Besides the isolation properties shown in Figure 18, it also deserves to examine the influence of the value of i on the ECCs between antennas. In Figure 6, the ECCs for all possible two-antenna pairs have been calculated from simulated

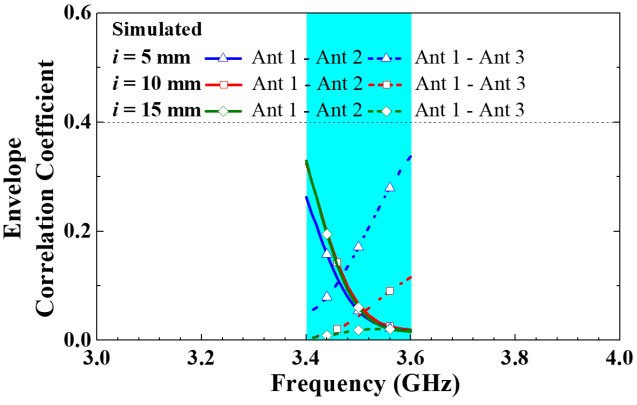

FIGURE 18. Simulated ECCs between selected antennas for different values of *i*.

and measured complex radiation patterns. Although the pair of Ants 1 and 2 (i.e., the first dual-slot-antenna unit) is geometrically the same as the pair of Ants 3 and 4 (i.e., the second dual-slot-antenna unit), the former is not identical to the latter if their surroundings are considered. In fact, the former is closer to the top edge of the FR4 substrate, and we should not expect to have the same intra-unit ECCs for the two dual-slot-antenna units. Similarly, we should not expect to have the same inter-unit ECCs for the pair of Ants 1 and 3 (1 and 4) and the pair of Ants 2 and 4 (2 and 3) if their surroundings are considered. Among all these sets of ECCs, the largest intra-unit ECCs occur for the pair of Ants 1 and 2, and the largest inter-unit ECCs occur for the pair of Ants 1 and 3. Hence, for simplicity, we will show in Figure 18 how the simulated ECCs for these two two-antenna pairs are affected by the separation distance i. It can be seen that the worst inter-unit ECC of the pair of Ants 1 and 3 at 3.6 GHz drops dramatically from 0.35 to 0.12 and then to 0.02 as i is changed from 5 mm to 10 mm and then to 15 mm, respectively. However, the worst intra-unit ECC of the pair of Ants 1 and 2 at 3.4 GHz is 0.27 for $i = 5$ mm, and is only slightly increased to 0.323 for both $i = 10$ and 15 mm. That the two intra-unit ECC curves for $i = 10$ and 15 mm are almost the same indicates that as the separation distance is large enough, the ECCs of the first dual-slot-antenna unit will not be affected by the second dual-slot-antenna unit, which is of no surprise. From the above results, $i = 10$ mm is expected to be the compromised parameter for achieving compactness and reasonably low inter- and intra-unit ECCs. In short, one cannot declare that a design is successful by simply checking the impedance matching and isolation. By examining Figures 16, 17, and 18, we can easily conclude that among the three values of i one should select 10 mm because the corresponding MIMO antenna system is the most compact one that can meet the impedance-matching, isolation, and ECC criteria at the same time.

In our design, the location of the operating band is mainly determined by the length of the L-shaped quarter-wavelength open-ended slot. To see this result, we will consider the MIMO antenna system where only the first dual-slot-antenna unit is present. Let the length of the longer section of the L-shaped open-ended slot be denoted by a with the ungrounded resonator removed and all other structural dimensions fixed. Figure 19 shows the reflection coefficients for three different values of a, i.e., 12, 13, and 14 mm. As expected, the larger the value of a, the longer the open-ended slot, and the lower the operating band. Among the three dual-slot-antenna units, the one with $a = 13$ mm produces the desired operating band. Hence, $a = 13$ mm is chosen in our design.

Finally, we will examine how the length of the unground strip resonator affects the S-parameters. For that purpose, let the length of the two outermost sections of the double-hook-shaped strip resonator be denoted by b with all other structural parameters fixed. Figure 20 shows the S-parameters for three different values of b, i.e., 4, 8, and 12 mm. Observe that if the value of b increases, the corresponding dip frequencies of

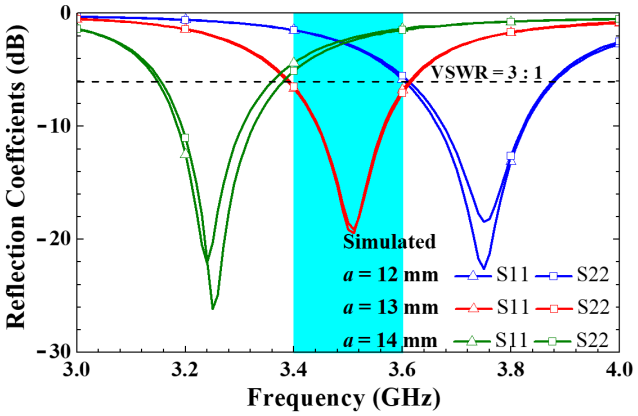

FIGURE 19. Simulated reflection coefficients for three different values of the parameter *a*.

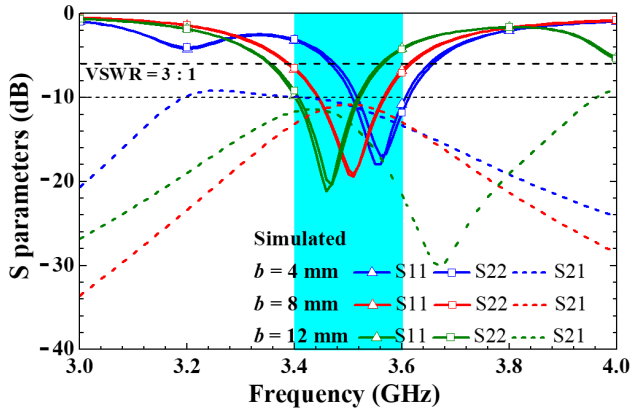

FIGURE 20. Simulated *S*-parameters for three different values of the parameter *b*.

the $|S_{11}|$ and $|S_{22}|$ curves decrease. This implies that both the slots and the ungrounded strip resonator contribute to the radiation. However, these reflection-coefficient dip frequencies are more sensitive to the length of the open-ended slot than to that of the ungrounded resonator if the reflection-coefficient curves in Figures 19 and 20 are compared. This suggests that the length of the open-ended slot plays the major role in determining the operating band and that of the ungrounded resonator plays the secondary. Hence, the ungrounded resonator can possibly be varied to fine-tune the operating band. Among the three dual-slot-antenna units, the ones with $b = 8$ and 12 mm give satisfactory isolations in 3400–3600 MHz. However, the one with $b = 12$ mm does not result in the required operating band. Hence, $b = 8$ mm is selected in our design.

E. LIQUID CRYSTAL DISPLAY AND HAND EFFECT

The case with a liquid crystal display (LCD) can also be studied [11], [12]. The LCD made of glass with dielectric constant 7 and loss tangent 0.02 has overall dimensions of 200 mm × 150 mm × 1 mm. Simulated S-parameters and antenna efficiencies are presented in Figures 21 and 22,

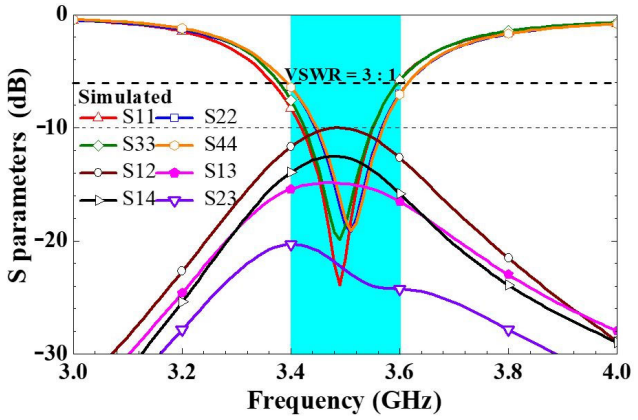

FIGURE 21. Simulated S-parameters for the proposed antenna system with an LCD.

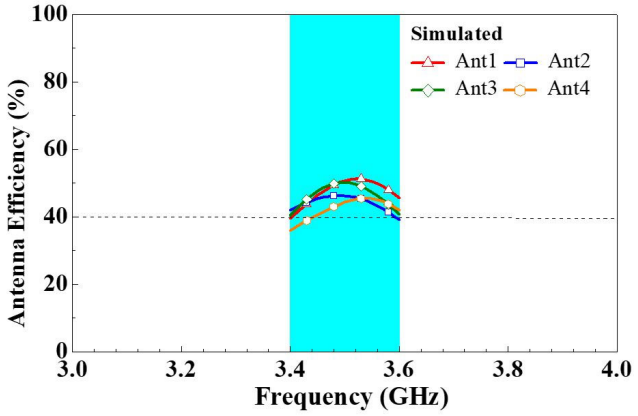

FIGURE 22. Simulated antenna efficiency for the proposed antenna system with an LCD.

respectively. It is seen that the simulated *S*-parameters for the case with an LCD are roughly the same as those for the case without an LCD in Figure 4. Simulated antenna efficiencies with an LCD in Figure 22 and measured antenna efficiencies without an LCD in Figure 8 are also very similar.

The case with the user's hand holding a mobile device has been studied in [11], [12]. In what follows we will carry out the same study. The SAR simulation model with the user's hand and SAR values for the 1-g hand tissue for the proposed MIMO antenna system are shown in Figure 23. Simulated results for the user's hand effects are obtained using SEMCAD [19]. The SAR values are tested using an input power of 21 dBm for three frequencies (3400, 3500, and 3600 MHz) in the sub-6-GHz band. It is observed that over the operating band, the obtained SAR values are all well below the SAR limit of 1.6 W/kg for the 1.0-g hand tissue [20]. These results indicate that the proposed MIMO antenna system is promising for practical applications. The simulated return loss and antenna efficiency at the testing frequencies are given in TABLE 2. It is seen that both the simulated results for the cases with and without the user's hand are generally the same. That is, effects of the user's

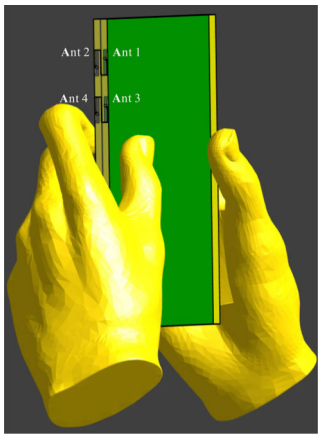

Frequncy (MHz)	3400	3500	3600
1-g SAR (W/kg)	0.37	0.47	0.56
Power (dBm)	21	21	21

FIGURE 23. SAR simulation model with the user's hand and the simulated SAR values for 1-g hand tissue for the proposed antenna system.

TABLE 2. SEMCAD-simulated return loss and antenna efficiency at three testing frequencies without and with the user's hand.

Frequncy (MHz)			3400	3500	3600
Return loss (dB)	w/o hand	Ant 1	6.32	9.65	11.45
		Ant 2	7.56	12.53	10.55
		Ant 3	8.16	13.93	9.29
		Ant 4	7.45	10.72	9.77
	with hand	Ant 1	6.62	10.09	10.06
		Ant 2	7.46	12.4	10.67
		Ant 3	8.87	12.05	8.81
		Ant 4	6.8	9.81	10.09
Efficiency (%)	w/o hand	Ant 1	41.23	51.57	44.86
		Ant 2	39.38	45.67	41.6
		Ant 3	37.56	49.68	43.78
		Ant 4	37.96	45.52	42.08
	with hand	Ant 1	37.33	44.85	34.91
		Ant 2	34.7	39.45	35.58
		Ant 3	22.94	31.26	27.36
		Ant 4	26.88	32.18	28.85

hand on the impedance matching of the antenna are quite small. However, the user's hand affects the antenna efficiency more than the impedance matching. The antenna efficiencies of Ants 1 and 2 with the user's hand are about 5–10% lower than those without. On the other hand, Ants 3 and 4 with the user's hand exhibits a larger reduction of 10–15% in antenna efficiency when compared to those without. This is because Ants 3 and 4 are closer to the user's hand than are Ants 1 and 2.

Figure 24 shows the simulated ECCs for the proposed antenna system with the user's hand. It can be clearly seen that the simulated ECCs with the user's hand are slightly changed and the maximum ECC is smaller as compared with the case without the user's hand in Fig. 6(a). The trend is the same as that in [21].

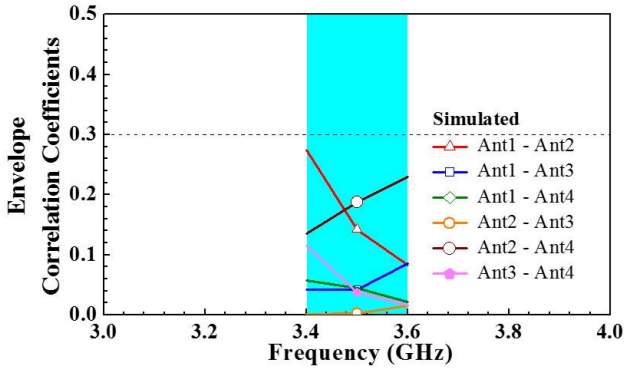

FIGURE 24. Simulated ECCs for the proposed antenna system with user's hand.

III. CONCLUSION

A four-element MIMO slot-antenna system has been designed for 5G tablets. This system consists of two 13.6 $\times$ 7 mm^2 dual-slot-antenna units separated by 10 mm. This MIMO slot-antenna system can produce an operating band that is wide enough to cover the desired 3400–3600 MHz frequency band required by 5G. In the operating band, the measured isolations are larger than 11 dB, and the measured antenna efficiencies are larger than 40%, which are good enough for practical 5G applications. The MIMO slot-antenna system can be constructed on the side-edge frame of a table without the need to leave any clearance in the system ground plane, and hence is highly suitable for tablets with a large display-to-body ratio.

ACKNOWLEDGMENT

The authors would like to thank Prof. Min-Hua Ho, the Graduate Institute of Communications Engineering, National Changhua University of Education, Changhua, Taiwan, ROC, for valuable discussion on transmission dips that can be observed in some weak transmission-coefficient curves in this article.

REFERENCES

[1] Y.-L. Ban, C. Li, C.-Y.-D. Sim, G. Wu, and K.-L. Wong, "4G/5G multiple antennas for future multi-mode smartphone applications," *IEEE Access*, vol. 4, pp. 2981–2988, Jul. 2016.
[2] K.-L. Wong and J.-Y. Lu, "3.6-GHz 10-antenna array for MIMO operation in the smartphone," *Microw. Opt. Technol. Lett.*, vol. 57, no. 7, pp. 1699–1704, Jul. 2015.
[3] Y. Li, C.-Y.-D. Sim, Y. Luo, and G. Yang, "Multiband 10-antenna array for Sub-6 GHz MIMO applications in 5-G smartphones," *IEEE Access*, vol. 6, pp. 28041–28053, Jun. 2018.
[4] K.-L. Wong and L.-Y. Chen, "Dual-inverted-F antenna with a decoupling chip inductor for the 3.6-GHz LTE operation in the tablet computer," *Microw. Opt. Technol. Lett.*, vol. 57, no. 9, pp. 2189–2194, Sep. 2015.
[5] S.-W. Su, C.-T. Lee, and S.-C. Chen, "Very-Low-profile, triband, two-antenna system for WLAN notebook computers," *IEEE Antennas Wireless Propag. Lett.*, vol. 17, no. 9, pp. 1626–1629, Sep. 2018.
[6] K. L. Wong, B. W. Lin, and S. E. Lin, "High-isolation conjoined loop MIMO antennas for the 5G tablet devices," *Microw. Opt. Technol. Lett.*, vol. 61, pp. 111–119, Jan. 2019.
[7] K.-L. Wong and H.-J. Chang, "Hybrid dual-antenna for the 3.6-GHz LTE operation in the tablet computer," *Microw. Opt. Technol. Lett.*, vol. 57, no. 11, pp. 2592–2598, Nov. 2015.
[8] K.-L. Wong, C.-Y. Tsai, and J.-Y. Lu, "Two asymmetrically mirrored gap-coupled loop antennas as a compact building block for eight-antenna MIMO array in the future smartphone," *IEEE Trans. Antennas Propag.*, vol. 65, no. 4, pp. 1765–1778, Apr. 2017.
[9] K.-L. Wong, B.-W. Lin, and B. W.-Y. Li, "Dual-band dual inverted-F/loop antennas as a compact decoupled building block for forming eight 3.5/5.8-GHz MIMO antennas in the future smartphone," *Microw. Opt. Technol. Lett.*, vol. 59, no. 11, pp. 2715–2721, Nov. 2017.
[10] K. L. Wong, Y. H. Chen, and W. Y. Li, "Decoupled compact ultra-wideband MIMO antennas covering 3300 6000 MHz for the fifth-generation mobile and 5GHz-WLAN operations in the future smartphone," *Microw. Opt. Technol. Lett.*, vol. 60, pp. 2345–2351, Oct. 2018.
[11] M. Abdullah, S. H. Kiani, L. F. Abdulrazak, A. Iqbal, M. A. Bashir, S. Khan, and S. Kim, "High-performance multiple-input multiple-output antenna system for 5G mobile terminals," *Electronics*, vol. 8, no. 10, p. 1090, Sep. 2019.
[12] M. Abdullah, S. H. Kiani, and A. Iqbal, "Eight element multiple-input multiple-output (MIMO) antenna for 5G mobile applications," *IEEE Access*, vol. 7, pp. 134488–134495, 2019.
[13] J.-Y. Sze, K.-L. Wong, and C.-C. Huang, "Coplanar waveguide-fed square slot antenna for broadband circularly polarized radiation," *IEEE Trans. Antennas Propag.*, vol. 51, no. 8, pp. 2141–2144, Aug. 2003.
[14] T. C. Edwards and J. B. Steer, *Foundations for Microstrip Circuit Design*, 4th ed. London, U.K.: Wiley, 2016.
[15] *Corporation HFSS*. Accessed: Apr. 16, 2019. [Online]. vailable:http://www.ansys.com/products/electronics/ansys-hfss
[16] Y. A. S. Dama, R. A. Abd-Alhameed, S. M. R. Jones, D. Zhou, N. J. McEwan, M. B. Child, and P. S. Excell, "An envelope correlation formula for (N, N) MIMO antenna arrays using input scattering parameters, and including power losses," *Int. J. Antennas Propag.*, vol. 2011, pp. 1–7, Aug. 2011.
[17] R. G. Vaughan and J. B. Andersen, "Antenna diversity in mobile communications," *IEEE Trans. Veh. Technol.*, vol. 36, no. 4, pp. 149–172, Nov. 1987.
[18] C.-Y. Tsai, K.-L. Wong, and W.-Y. Li, "Experimental results of the multi-gbps smartphone with 20 multi-input multi-output (MIMO) antennas in the 20$\times$12 MIMO operation," *Microw. Opt. Technol. Lett.*, vol. 60, no. 8, pp. 2001–2010, Aug. 2018.
[19] *SPEAG SEMCAD*. Accessed: Mar. 19, 2019. [Online]. Available: http://www.semcad.com
[20] *IEEE Standard for Safety Levels With Respect to Human Exposure to Electric, Magnetic, and Electromagnetic Fields, 0 Hz to 300 GHz*, Standard C95.1-2019. Accessed: Jun. 2, 2020. [Online]. vailable:. [Online]. Available: https://standards.ieee.org/standard/C95_1-2019.html
[21] K.-L. Wong, Y.-C. Chen, and W.-Y. Li, "Four LTE low-band smartphone antennas and their MIMO performance with user's hand presence," *Microw. Opt. Technol. Lett.*, vol. 58, pp. 2046–2052, Sep. 2016.